PERGAMON

International Journal of Solids and Structures 36 (1999) 4963–4974

INTERNATIONAL JOURNAL OF SOLIDS and STRUCTURES

Young's modulus interpreted from plane compressions of geomaterials between rough end blocks

K.T. Chau

Department of Civil and Structural Engineering, The Hong Kong Polytechnic University, Yuk Choi Road, Hung Hom, Kowloon, Hong Kong, China

Received 10 April 1997; accepted 22 July 1998

Abstract

This note derives an approximate expression of the true Young's modulus of a rectangular solid under plane compression between two rough end blocks, provided that the Poisson's ratio v of the solid is known. The friction between the loading platens and the ends of the specimen is assumed to be large enough to restrain slippage at the contact. By using the function space concept of Prager and Synge (1947), a correction factor λ with calculable error is obtained which can be multiplied to the apparent Young's modulus (i.e., the one obtained by assuming uniform stress field) to yield the true Young's modulus; it is evaluated numerically for $0 \leqslant v \leqslant 0.49$ and $0 \leqslant \eta \leqslant 3$ (where $\eta = b/h$ with b and h being the half width and half length of the specimen). In general, λ increases with v and η for both plane strain and plane stress compressions. Within this range of v and η, λ may vary from 0.37–1.0 for the plane strain case and from 0.84–1.0 for the plane stress case. Thus, the assumption of uniform stress field may lead to erroneous interpretation of the Young's modulus. When the special case of $v = 1/3$ and $\eta = 1$ is considered, we obtain $\lambda = 0.9356$, which compares well with 0.9359 obtained by Greenberg and Truell (1948).

1. Introduction

Although plane strain compression is not a standard laboratory test for geomaterials, its popularity increases in recent years, partly because plane strain condition is more conducive to the formation of strain localization in geomaterials (e.g., Rudnicki and Rice, 1975) and the prediction of strain localization is a useful way to calibrate constitutive models, and partly because plane strain states are commonly encountered in geotechnical engineering problems (e.g., Jaeger and Cook, 1979). For examples, plane strain compression has been used in studying the problems of strain localization or fracture formation in rocks by Brown (1974), Stavropoulou (1982), Wawersik et al. (1990), Ord et al. (1991) and Tillard-Ngan et al. (1992), and in rock-like materials by Labuz et al. (1996). The plane strain compression apparatus has also been developed for soil testing (e.g., Vardoulakis and Goldscheider, 1981; Drescher et al. 1990).

0020-7683/99/$ - see front matter
PII: S0020-7683(98)00274-1

Most of the previous theoretical studies for plane strain test have been on the instabilities of the tested solids; they include the stability analyses for metal-like materials by Ariaratnam and Dubey (1969), Dubey (1975), Hill and Hutchinson (1975) and Young (1976), for soil-like materials by Vardoulakis (1981) and Bardet (1991), and for rock-like materials by Needleman (1979), Chau and Rudnicki (1990) and Chau (1994). To make the problem mathematically tractable, all of these analyses assume that the rectangular blocks are loaded by a uniform velocity with no end friction. Although various experimental techniques have been proposed to reduce the end friction (e.g., Labuz and Bridell, 1993), end friction between the loading platens and the specimen inevitably exists in most of the usual experimental set-up.

Friction between loading machines and the tested specimen has long been recognized to exist. However, most of the previous attention has been paid to axisymmetric compression of cylinders, frictional effect has not been considered thoroughly for the plane strain compression tests. For example, Filon's (1902) pioneering analysis for the nonuniform stress field inside a cylindrical solid of finite length due to end friction has inspired a series of subsequent and more recent theoretical analyses by Pickett (1944), Balla (1960a,b), Peng (1971, 1973), Brady (1971), Al-Chalabi (1972), Al-Chalabi and Huang (1974), and Al-Chalabi et al. (1974). However, as discussed by Chau (1997), except the original analysis by Filon (1902) none of these studies attempts to calculate the correction factor for the true Young's modulus. Extending the work by Edelman (1949) and applying the function space concept of Prager and Synge (1947), Chau (1997) has re-considered the frictional effect on the apparent Young's modulus of cylindrical specimens and derived an approximate solution for the correction factor λ, which can be multiplied by the apparent Young's modulus to yield the true Young's modulus.

The main purposes of this short paper is to derive a correction factor λ for the true Young's modulus E of a rectangular block of dimension $2b \times 2h$, by employing the Prager–Synge (1947) function space approach. When friction between the loading platens and the specimen is negligible or the stress field inside the specimen is uniform, the true Young's modulus E coalesces with the apparent Young's modulus $\bar{E}$, which equals $Fh(1-\nu^2)/(2b\delta)$ for plane strain compression and equals $Fh/(2b\delta)$ for plane stress compression [where F is the applied force per unit thickness along the x_2 direction (see Fig. 1), δ half of the axial deformation of the specimen along the direction of F, and ν the Poisson's ratio of the specimen]. However, when friction appears at the contact between the loading platens and the specimen, a correction factor λ has to be multiplied by $\bar{E}$ in order to yield E (i.e., $E = \lambda\bar{E}$).

The analysis to be discussed here can be considered as an extension of the theoretical analysis by Greenberg and Truell (1948), which only considers the case of Poisson ratio being 1/3 (i.e., $\nu = 1/3$) and the case of square specimen (i.e., $b/h = 1$). However, as mentioned previously, one of the major reasons why plane strain test is adopted is to capture the onset of strain localization or shear band formation, but, as mentioned in Needleman (1979) and Chau and Rudnicki (1990), an additional kinematic constraint that $\tan\theta \geqslant h/b$ has to be imposed (where θ is the angle between the normal of the shear band to the x_2 axis). Experimental studies on plane strain compression of rock specimens suggest that θ ranges from 55–72.5° (e.g., Wawersik et al., 1990; Ord et al., 1991; Tillard-Ngan et al. 1992); this range of θ together with the kinematic constraint, yields an aspect ratio b/h of being smaller than 0.7 to 0.32. Thus, for practical purposes, the result by Greenberg and Truell (1947) for the case of $b/h = 1$ is rather restrictive. Therefore, we will consider in this paper the correction factor λ for all combinations of b/h and ν within the practical range. In

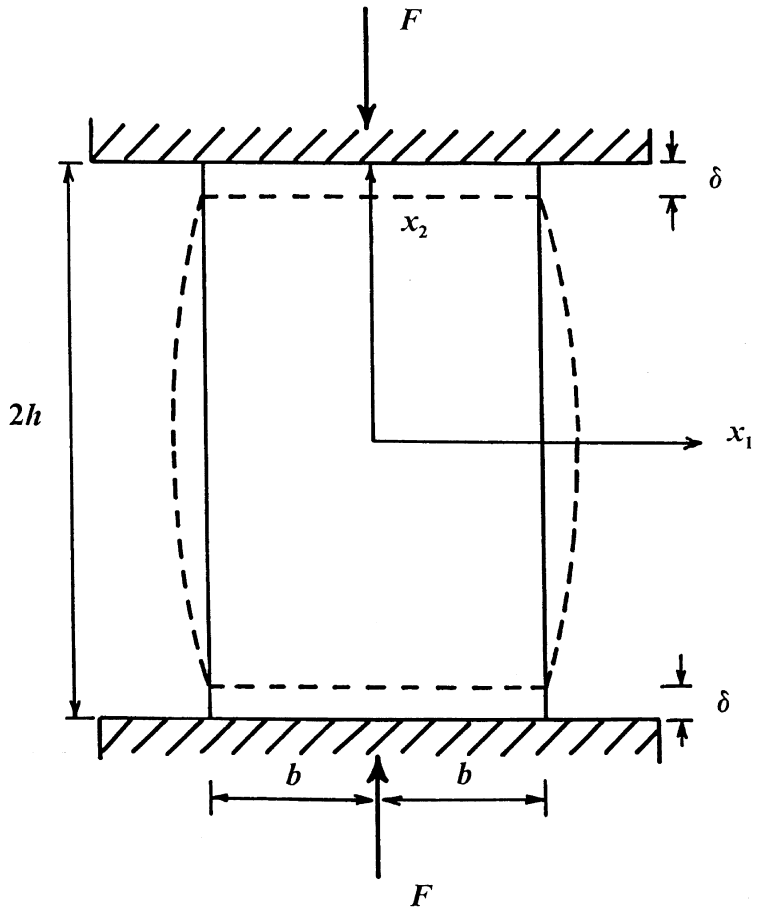

Fig. 1. A sketch for the possible deformed shape (dotted lines) of a rectangular block of width $2b$ and height $2h$ under plane compression between two rough ends, comparing to the initial undeformed shape (solid lines). The origin of the x_1-x_2 coordinate is at the center of the block, the applied force per unit thickness is F, and the total vertical deformation is 2δ.

addition, the present analysis considers both plane strain and plane stress compressions, whilst Greenberg and Truell's (1948) analysis applies only to plane strain case. However, only the cases of sufficient large contact friction are considered here, that is, partial contact slippage is neglected in our problem.

Note that another limitation of the present approach is that Poisson's ratio of the solid has to be known in advance. As discussed by Chau (1997), this limitation should not be too restrictive, since the uniaxial compression tests by Peng (1971) on cylindrical specimens of steel and Chelmsford granite show that the axial and circumferential strains measured at the mid-level are insensitive to the end friction and equal, without appreciable error, to those with zero end friction. Thus, the Poisson's ratio can simply be found from the circumferential and axial strains measured at the mid-level, regardless of the end conditions.

Since the analysis is analogous to that by Greenberg and Truell (1948), only the main differences and the essential procedure of the analysis is summarized in here.

2. Governing equations for the problem

If no special treatment is applied to the loading platens of a compression machine, friction inevitably exists at the contact between the rectangular specimen and the loading platens. Such friction will lead to nonuniform deformation, and hence nonuniform stress field, inside the specimen. Consequently, the apparent Young's modulus of $\bar{E}$ obtained by assuming uniform stress field inside the specimen may lead to erroneous estimation of the true Young's modulus E. Figure 1 sketches a typical deformed shape of the rectangular block of original dimension of $2b \times 2h$ under two-dimensional compression when the end friction is large enough to restrain contact slippage.

The solids considered here are assumed to be isotropic and elastic, and the Poisson's ratio is a known constant, as discussed in the Introduction. In particular, the following two-dimensional Hooke's law between the stress tensor (σ) and strain tensor (ε) applies (e.g., Karasudhi, 1991):

$$\sigma_{ij} = \frac{\mu}{\kappa - 1}[2(\kappa - 1)\varepsilon_{ij} + (3 - \kappa)\delta_{ij}\varepsilon], \tag{1}$$

where $i, j = 1, 2$; and $\varepsilon = \varepsilon_{11} + \varepsilon_{22}$ is the in-plane volumetric strain, μ is the shear modulus and κ equals $3 - 4\nu$ for plane strain and $(3 - \nu)/(1 + \nu)$ for plane stress. The Kronecker delta function δ_{ij} equals zero if $i \neq j$ and one if $i = j$. The apparent Young's modulus [i.e., $\bar{E} = Fh(1 - \nu^2)/(2b\delta)$ for plane strain and $\bar{E} = Fh/(2b\delta)$ for plane stress] given in the Introduction can be derived by assuming a uniform axial stress field [i.e., $\sigma_{22} = F/(2b)$ and $\sigma_{11} = 0$] and axial strain of $\varepsilon_{22} = \delta/h$. Thus, (1) can be used to yield

$$\frac{\sigma_{22}}{\varepsilon_{22}} = \frac{4\bar{E}}{(1 + \nu)(1 + \kappa)} = \frac{Fh}{2\delta b}. \tag{2}$$

Therefore, it follows immediately from the second of (2) that $\bar{E} = Fh(1 - \nu^2)/(2b\delta)$ for plane strain and $\bar{E} = Fh/(2b\delta)$ for plane stress. For the coordinate system shown in Fig. 1, the end displacement conditions of our compression problem are:

$$u_2(x_1, \pm h) = \mp \delta, \quad u_1(x_1, \pm h) = 0; \tag{3}$$

and the traction free boundary conditions on the vertical surfaces are

$$\sigma_{11}(\pm b, x_2) = 0, \quad \sigma_{12}(\pm b, x_2) = 0. \tag{4}$$

The total strain energy for our compression problem equals the external work done on the specimen or is $F\delta$. That is, $\frac{1}{2}F\delta$ on both the upper and lower ends of the specimen if the force F is applied quasi-statically.

Now, our main task is to obtain an approximation for λ such that the true Young's modulus E can be estimated by $\lambda\bar{E}$, where $\bar{E}$ is the apparent Young's modulus obtained from the compression test by assuming zero end friction.

3. Prager–Synge (1947) function space concept

As illustrated by Greenberg and Truell (1948), the function space concept of Prager and Synge (1947) provides a powerful tool to estimate the true Young's modulus of a solid under plane compression, even though nonuniform stresses may exist in the rectangular block. In particular, Prager and Synge (1947) noticed that any state of stress for a particular problem of elastic solids can be considered as a point or vector $\mathbf{S}$ in a function space of states. Since displacement boundary conditions (3) are prescribed on the top and bottom of the specimen, the present problem corresponds to the so-called *Displacement Boundary Conditions* (DBC) cases discussed by Prager and Synge (1947). An approximation of λ with calculable error can be found since the strain energy for the exact solution can be bounded by functions of sequences of fictitious states, as the unknown solution $\mathbf{S}$ is located on a hypercircle with determinable center and radius. More specifically, Prager and Synge (1947) showed that a fictitious state $\mathbf{S}^*$ called the *completely associated state*, which satisfies only the compatibility equation and the displacement boundary conditions (3), and the actual solution $\mathbf{S}$ (or the *natural* state) will form a hypersphere such that vector $\mathbf{S}^*$ would be its diameter and vector $\mathbf{S}$ would be on the surface of the hypersphere. A sequence of fictitious states called the *homogeneous associated states* $\mathbf{S}'$, which satisfy the compatibility equation and the homogeneous displacement boundary conditions (obtained by setting the right hand sides of (3) zero) can always be added to $\mathbf{S}^*$ such that the above observation remains valid. When another sequence of fictitious states $\mathbf{S}''$ called the *complimentary states*, which satisfy the equations of equilibrium and the stress boundary condition (4), is assumed, the natural state $\mathbf{S}$ will lie on a hyperplane normal to $\mathbf{S}''$. The intersection of these hypersphere and hyperplane then forms a hypercircle on which the unknown $\mathbf{S}$ must lie. By purely geometrical consideration, Prager and Synge (1947) showed that the strain energy of the solution $\mathbf{S}$ is bounded by the size of the hypercircle in the function space as:

$$\sum_{q=1}^{n} (\mathbf{S}^* \cdot \mathbf{I}''_q)^2 \leqslant S^2 \leqslant S^{*2} - \sum_{p=1}^{m} (\mathbf{S}^* \cdot \mathbf{I}'_p)^2, \tag{5}$$

where m and n are the numbers of the homogeneous associated states and complimentary states used for $\mathbf{S}'_p$ and $\mathbf{S}''_q$, with both of them should be chosen to be linearly independent. In addition, the following definition for the scalar product between any two states (say $\mathbf{S}$ and $\mathbf{S}'$)

$$S \cdot S' = \int \sigma_{ij} \varepsilon'_{ij} \, \mathrm{d}V, \tag{6}$$

where σ_{ij} is the stress tensor corresponding to the state $\mathbf{S}$ and ε'_{ij} the strain tensor corresponding to $\mathbf{S}'$. The integration on the right-hand side is done over the entire volume. The orthonormal sets for the states $\mathbf{S}'$ and $\mathbf{S}''$ are denoted by $\mathbf{I}'_p$ and $\mathbf{I}''_q$ ($p = 1, \ldots m$ and $q = 1, \ldots n$), and defined by

$$\mathbf{I}'_p \cdot \mathbf{I}'_r = \delta_{pr}, \quad \mathbf{I}''_q \cdot \mathbf{I}''_r = \delta_{qr}. \tag{7}$$

Attractive features of the present approach include: the upper bound decreases whilst the lower bound increases as more terms are added to (5) (i.e., m and n increase); and, the maximum error of the strain energy of any proposed approximation is measurable in terms of distance in the function space. This function space concept is now applied to our problem of plane compression.

4. The lower and upper bounds for λ

As remarked earlier, strain energy of our compression problem equals the external work done $F\delta$, which also equals half of S^2. Substitution of this result into (5) yields the following lower and upper bounds for S^2

$$L_n \frac{Ebh}{2(1+v)}\left(\frac{\delta}{h}\right)^2 \leqslant 2F\delta \leqslant U_m \frac{Ebh}{2(1+v)}\left(\frac{\delta}{h}\right)^2, \tag{8}$$

where L_n and U_m are the normalized lower and upper bounds of the strain energy, and are defined as:

$$L_n = \frac{1}{\mu bh}\left(\frac{h}{\delta}\right)^2 \sum_{q=1}^{n} (\mathbf{S}^* \cdot \mathbf{I}_q'')^2, \quad U_m = \frac{1}{\mu bh}\left(\frac{h}{\delta}\right)^2 \left\{ S^{*2} - \sum_{p=1}^{m} (\mathbf{S}^* \cdot \mathbf{I}_p')^2 \right\}. \tag{9}$$

Alternatively, if F and δ are known, (8) can be rearranged to obtain the upper and lower bounds for the Young's modulus:

$$\frac{4F(1+v)}{U_m b}\left(\frac{h}{\delta}\right) \leqslant E \leqslant \frac{4F(1+v)}{L_n b}\left(\frac{h}{\delta}\right). \tag{10}$$

Substitution of the apparent Young's modulus given in (2) into (10) yields

$$\lambda_L = \frac{32}{U_m(1+\kappa)} \leqslant \lambda = \frac{E}{\bar{E}} \leqslant \lambda_U = \frac{32}{L_n(1+\kappa)}, \tag{11}$$

4.1. Approximation I

A simple estimation for the correction factor λ is the average of the upper and lower bounds, that is

$$E = \lambda \bar{E} = \tfrac{1}{2}(\lambda_L + \lambda_U)\bar{E}, \tag{12}$$

where λ_U and λ_L are defined in (11). However, as will be shown later in Fig. 2, when the limit $\eta \to 0$ is considered, this prediction for λ does not approach 1; and it is obvious that (12) is only one of the many possible estimations for λ within the upper and lower bounds λ_U and λ_L. Therefore, a more refined approximation is proposed next.

4.2. Approximation II

Based upon the comparison with the analytical solution by Watanabe (1998), Chau (1998) proposed the following more refined choice for λ such that the appropriate limit at $\eta = 0$ can be achieved:

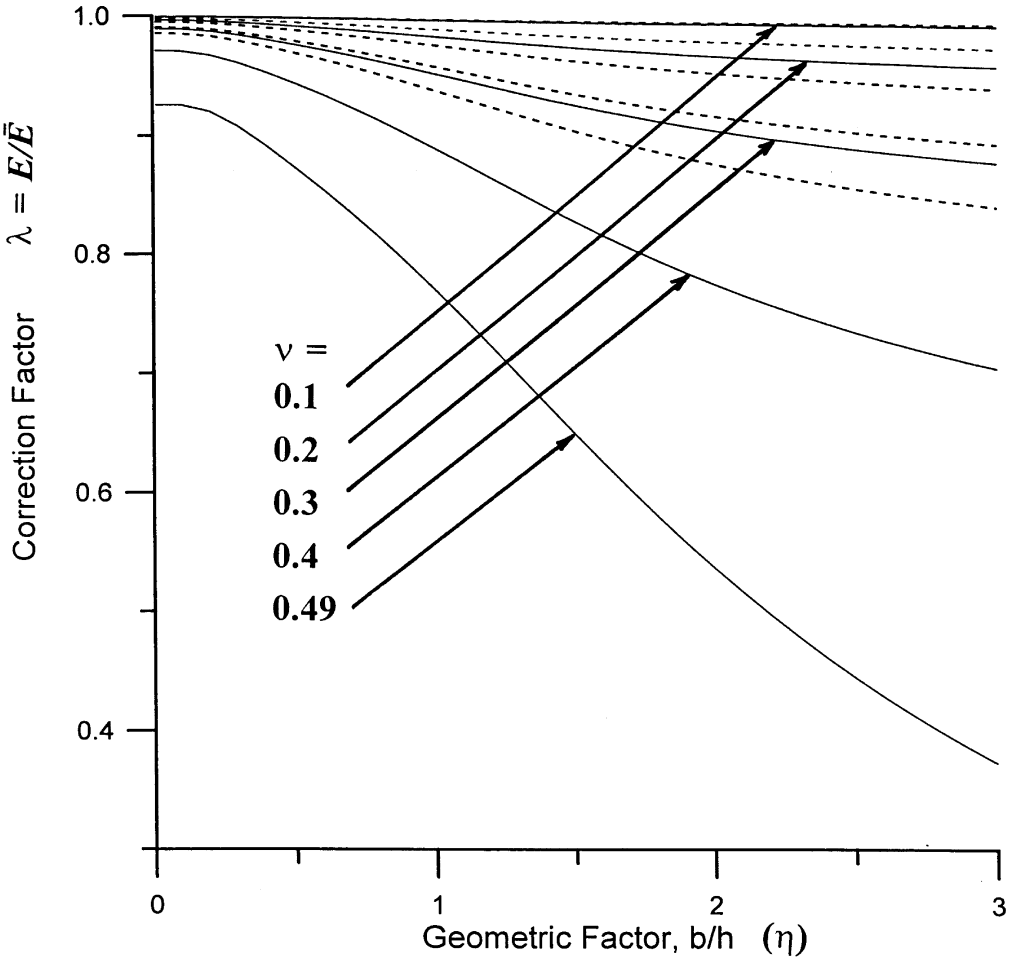

Fig. 2. The correction factor $\lambda = E/\bar{E}$ vs the geometric ratio $\eta = b/h$ for the Approximation I given in (12) for various values of the Poisson's ratio v under the plane strain (solid lines) and the plane stress (dotted lines) compressions.

$$\begin{aligned} \lambda &= \lambda_U(1-\eta)+\lambda_L\eta \quad 0 \leqslant \eta \leqslant \tfrac{1}{2} \\ \lambda &= \tfrac{1}{2}(\lambda_U+\lambda_L) \qquad\quad \eta \geqslant \tfrac{1}{2} \end{aligned} \tag{13}$$

4.3. Selection of $\mathbf{S}^*$, $\mathbf{S}'$ and $\mathbf{S}''$

Since the procedure in obtaining the appropriate states for $\mathbf{S}^*$, $\mathbf{S}'$, and $\mathbf{S}''$ have been discussed in Chau (1997), we only summarize the corresponding displacement fields for $\mathbf{S}^*$ and $\mathbf{S}'$ and the Airy stress function ψ for $\mathbf{S}''$ being used here in Table 1. For the sake of completeness and easy reference, Tables 2 and 3 also compile the scalar products between $\mathbf{S}^*$ and $\mathbf{S}'$ and between $\mathbf{S}^*$ and $\mathbf{S}''$ respectively. With these scalar products, the upper and lower bounds for energy L_n and U_m can

Table 1
The displacements for the completely associated state $\mathbf{S}^*$ and the homogeneous associated states $\mathbf{S}'_p$ ($p = 1, 2, \ldots, 5$), and the Airy stress function ψ for the complimentary states $\mathbf{S}''_q$ (q $= 1, 2, \ldots, 5$)

State	u_1	u_2	State	ψ/μ
$\mathbf{S}'_1$	$b\xi(1-\zeta^2)$	0	$\mathbf{S}''_1$	$-1/2b^2\xi^2$
$\mathbf{S}'_2$	0	$-h\zeta(1-\zeta^2)$	$\mathbf{S}''_2$	$-\xi^4b^2/12$
$\mathbf{S}'_3$	$b\xi^3(1-\zeta^2)$	0	$\mathbf{S}''_3$	$\frac{1}{2}\zeta^2h^2(1-\xi^2)^2$
$\mathbf{S}'_4$	0	$-\zeta(1-\zeta^2)\xi^2h$	$\mathbf{S}''_4$	$\frac{1}{4}\zeta^4h^2(1-\xi^2)^2$
$\mathbf{S}'_5$	$b\xi^3\zeta^2(1-\zeta^2)$	0	$\mathbf{S}''_5$	$\frac{1}{2}\zeta^2b^2(1-\xi^2)^2\xi^2$
$\mathbf{S}^*$	0	$-\zeta\delta$		

be obtained (see the procedure discussed in Greenberg and Truell, 1948), which, in turn, also leads to solution for λ by using (11–13). The numerical results are discussed next.

5. Numerical results

Using Approximation I, Fig. 2 plots the correction factor $\lambda = E/\bar{E}$ vs the geometric ratio $\eta = b/h$ for v ranging from 0.1–0.49. The dotted lines are the prediction of λ for plane stress compression while the solid lines are for plane stress compression. Similar to the prediction for compression of cylindrical specimens (Chau, 1997), the correction factor λ drops with both geometric ratio $\eta = b/h$ and Poisson's ratio v. That is, λ decreases, or deviates farther away from unity, as the specimen becomes shorter. Since the difference between λ and unity for plane strain case is substantially larger than that of the plane stress case, plane strain compression is more conducive to frictional effect than plane stress compression. Similar to the case of axisymmetric compression considered by Chau (1997), the correction factor λ converges to 1 as the Poisson's ratio approaches zero. As shown in Fig. 2, the apparent Young's modulus may lead to an error of up to 170% for thin and nearly incompressible materials (i.e., $v = 0.49$ and $\eta = 3$). Note that when $\eta \to 0$, the prediction by Approximation I does not converge to the proper limit of one; that is, no correction factor should be made for very long specimens, as the end friction effect becomes negligible.

Therefore, the more refined prediction for λ by Approximation II given in (13), are plotted in Fig. 3. Again, the solid and dotted lines are for the plane strain and plane stress cases respectively. As expected $\lambda \to 1$ as η approaches zero. We believe that this prediction should provide an improved estimation of λ over those given by (12) or in Fig. 2.

To check the validity of the present prediction, the special case of $v = 1/3$ and $\eta = 1$ is also considered, and we find that the correction factor λ for the Young's modulus is about 0.9356 with a maximum error of 1.0087%, which agrees well with the result of 0.9359 obtained by Greenberg and Truell (1948). For the case of plane strain compression, the maximum error for λ given in Figs 2 and 3 is always less than 2.5% for v up to 0.4, but increases to about 7% for $v = 0.49$ and $\eta = 3$; and, for the cases of plane stress compression, the maximum error for λ given in Figs 2 and

Table 2
The scalar products for $\mathbf{S}'_i \cdot \mathbf{S}'_j/(\mu bh)$ and $\mathbf{S}'_i \cdot \mathbf{S}^*/(\mu bh)$

State	$\mathbf{S}'_1$	$\mathbf{S}'_2$	$\mathbf{S}'_3$	$\mathbf{S}'_4$	$\mathbf{S}'_5$	$\mathbf{S}^*$
$\mathbf{S}'_1$	$\frac{32}{15}\left(\frac{1+\kappa}{\kappa-1}\right)+\frac{16}{9}\eta^2$	$\frac{16}{15}\left(\frac{\kappa-3}{\kappa-1}\right)$	$\frac{32}{15}\left(\frac{1+\kappa}{\kappa-1}\right)+\frac{16}{15}\eta^2$	$\frac{16}{45}\left(\frac{3\kappa-5}{\kappa-1}\right)$	$\frac{32}{105}\left(\frac{1+\kappa}{\kappa-1}\right)+\frac{16}{75}\eta^2$	$\frac{8}{3}\left(\frac{\kappa-3}{\kappa-1}\right)\left(\frac{\delta}{h}\right)$
$\mathbf{S}'_2$		$\frac{16}{5}\left(\frac{\kappa+1}{\kappa-1}\right)$	$\frac{16}{15}\left(\frac{\kappa-3}{\kappa-1}\right)$	$\frac{16}{15}\left(\frac{\kappa+1}{\kappa-1}\right)$	$\frac{16}{105}\left(\frac{3-\kappa}{\kappa-1}\right)$	0
$\mathbf{S}'_3$			$\frac{96}{25}\left(\frac{1+\kappa}{\kappa-1}\right)+\frac{16}{21}\eta^2$	$\frac{16}{75}\left(\frac{5\kappa-11}{\kappa-1}\right)$	$\frac{96}{175}\left(\frac{1+\kappa}{\kappa-1}\right)+\frac{16}{105}\eta^2$	$\frac{8}{3}\left(\frac{\kappa-3}{\kappa-1}\right)\left(\frac{\delta}{h}\right)$
$\mathbf{S}'_4$				$\frac{16}{25}\left(\frac{1+\kappa}{\kappa-1}\right)+\frac{128}{315\eta^2}$	$\frac{16}{525}\left(\frac{11-5\kappa}{\kappa-1}\right)$	0
$\mathbf{S}'_5$					$\frac{32}{175}\left(\frac{1+\kappa}{\kappa-1}\right)+\frac{176}{735}\eta^2$	$\frac{8}{15}\left(\frac{\kappa-3}{\kappa-1}\right)\left(\frac{\delta}{h}\right)$
$\mathbf{S}^*$	Sym.					$4\left(\frac{1+\kappa}{\kappa-1}\right)\left(\frac{\delta}{h}\right)$

Table 3
The scalar products for $\mathbf{S}''_i \cdot \mathbf{S}''_j/(\mu bh)$ and $\mathbf{S}''_i \cdot \mathbf{S}^*/(\mu bh)$

State	$\mathbf{S}''_1$	$\mathbf{S}''_2$	$\mathbf{S}''_3$	$\mathbf{S}''_4$	$\mathbf{S}''_5$	$\mathbf{S}^*$
$\mathbf{S}''_1$	$\frac{1}{2}(1+\kappa)$	$(1+\kappa)/6$	$4(3-\kappa)/15$	$4(3-\kappa)/15$	$4\eta^2(3-\kappa)/105$	$4\delta/h$
$\mathbf{S}''_2$		$(1+\kappa)/10$	$-4[3\eta^2(\kappa-3)+7(1+\kappa)]/(315\eta^2)$	$-2[7(\kappa+1)+10\eta^2(\kappa-3)]/(525\eta^2)$	$4[\eta^2(3-\kappa)-(1+\kappa)]/315$	$4\delta/3h$
$\mathbf{S}''_3$			$8\{40\eta^2[\eta^2(1+\kappa)+11-\kappa]+63(1+\kappa)\}/(1575\eta^4)$	$4\{4\eta^2[20\eta^2(1+\kappa)+3(53-7\kappa)]+45(1+\kappa)\}/(1575\eta^4)$	$8(1+\kappa)(40\eta^4+99)/(17325\eta^2)$	0
$\mathbf{S}''_4$				$2[(1+\kappa)(245+2016\eta^4)+240\eta^2(25-3\kappa)]/(11025\eta^4)$	$4(1+\kappa)(99+112\eta^4)/(24255\eta^2)$	0
$\mathbf{S}''_5$	Sym.				$(64\eta^4/15015+24/175)(\kappa+1)+64\eta^2(11-\kappa)/3465$	0

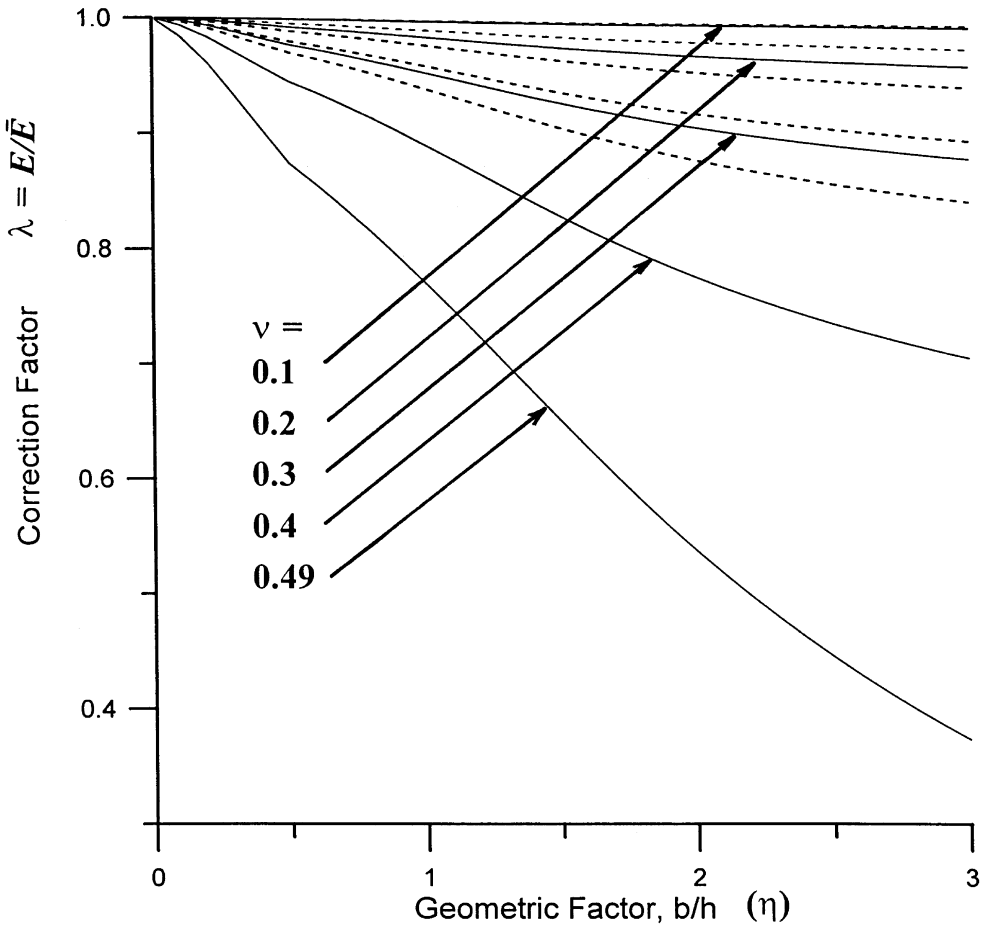

Fig. 3. The correction factor $\lambda = E/\bar{E}$ vs the geometric ratio $\eta = b/h$ for the Approximation II given in (13) for various values of the Poisson's ratio v under the plane strain (solid lines) and plane stress (dotted lines) compressions.

3 is always less than 0.8%. Therefore, the numerical results for λ given here should be reliably accurate for practical purposes.

6. Conclusion

By extending the analysis by Greenberg and Truell (1948) and by applying the function space concept of Prager and Synge (1947), we have obtained numerically the prediction for the correction factor λ, which can be multiplied by the *apparent* Young's modulus to yield the *true* Young's modulus, for Poisson's ratio (v) ranging from 0–0.49 and the geometric ratio $\eta = b/h$ from 0–3 (where b and h are the half width and half length of the rectangular solid). These ranges for η and v should include most of the conditions that we may encounter in practice. Similar to the case of axisymmetric compression (Chau, 1997), we find that the correction λ is always less than one; that

is, the Young's modulus is always being overestimated if there is friction between the loading platens and the specimen. For the parameters that we have used, λ may vary from 0.37–1. Thus, the usual assumption of uniform stress field may lead to erroneous value of the Young's modulus if end friction is not negligible. Generally speaking, λ decreases with η and v. The prediction of λ for the special case of $v = 1/3$ and $\eta = 1$ is obtained as 0.9356 with a possible maximum error of 1.0087%, which agrees well with the prediction of 0.9359 by Greenberg and Truell (1948). With the present approach the maximum error can always be reduced if more terms of the homogeneous associated states $\mathbf{S}'_p$ and complimentary states $\mathbf{S}''_q$ are added.

Acknowledgements

The work was supported by the Competitive Earmarked Research Grants from the RGC. I am grateful to Mr C.M. Lam for his helpful discussion.

References

Al-Chalabi, M., 1972. Discussion of S.D. Peng's paper 'On stresses within elastic cylinders loaded uniaxially and triaxially.' Int. J. Rock Mech. Min. Sci. & Geomech. Abstr. 9, 665.

Al-Chalabi, M., Huang, C.L., 1974. Stress distribution within circular cylinders in compression. Int. J. Rock Mech. Min. Sci. & Geomech. Abstr. 11, 45–56.

Al-Chalabi, M., McCormick, F.J., Huang, C.L., 1974. Strain distribution within compressed circular cylinders. Experimental Mech. 14, 497–501.

Ariaratnam, S.T., Dubey, R.N., 1969. Some cases of bifurcation in elastic–plastic solids in plane strain. Quart. Appl. Math. 27, 349–358.

Balla, A., 1960a. A new solution of the stress conditions in triaxial compression. Acta Tech. Hung. 28, 349–387.

Balla, A., 1960b. Stress conditions in triaxial compression. Proc. ASCE 86 (SM6), 57–84.

Bardet, J., 1991. Analytical solutions for the plane-strain bifurcation of compressible solids. J. Appl. Mech. 58, 651–657.

Brady, B.T., 1971. An exact solution to the radially end-constrained circular cylinder under triaxial loading. Int. J. Rock Mech. Min. Sci. 8, 165–178.

Brown, E.T., 1974. Fracture of rock under uniform biaxial compression. Advances in Rock Mechanics, Proc. 3rd Congr. ISRM, Denver, Colorado, pp. 111–117.

Chau, K.T., 1994. Halfspace instabilities and short wavelength bifurcations in cylinders and rectangular blocks. J. Appl. Mech. 61, 742–744.

Chau, K.T., 1997. Young's modulus interpreted from compression tests with end friction. J. Eng. Mech. ASCE 123, 1–7.

Chau, K.T., 1998. Author's closure to Discussion by S. Watanabe on 'Young's modulus interpreted from compression tests with end friction.' J. Eng. Mech. ASCE 124, 1171–1174.

Chau, K.T., Rudnicki, J.W., 1990. Bifurcations of compressible pressure-sensitive materials in plane strain tension and compression. J. Mech. Phys. Solids 38, 875–898.

Drescher, A., Vardoulakis, L., Han, C., 1990. A biaxial apparatus for testing soils. Geotech. Testing J. ASTM 13, 226–234.

Dubey, R.N., 1975. Thick Body Bifurcations of Elastic and Elastic/Plastic Solids in Plane Strain: A Correlation Study Using Principal Axes Technique. Special Publication, Solid Mechanics Division, University of Waterloo.

Edelman, F., 1949. On the compression of a short cylinder between rough end-blocks, Quart. Appl. Math 7, 334–337.

Filon, L.N.G., 1902. On the equilibrium of circular cylinders under certain practical systems of load. Phil. Trans. R. Soc. Lond. Series A 198, 147–233.

Greenberg, H.J., Truell, R., 1948. On a problem in plane strain. Quart. Appl. Math 6, 53–62.
Hill, R., Hutchinson, J.W., 1975. Bifurcation phenomena in the plane tension test. J. Mech. Phys. Solids 23, 239–264.
Jaeger, C.J., Cook, N.G.W., 1979. Fundamentals of Rock Mechanics, 3rd ed. Chapman and Hall, London.
Karasudhi, P., 1991. Foundations of Solid Mechanics. Kluwer Academic Publishers, Dordrecht.
Labuz, J.F., Bridell, J.M., 1993. Reducing frictional constraint in compression testing through lubrication. Int. J. Rock. Mech. Min. Sci. & Geomech. Abstr. 30, 451–455.
Labuz, J.F., Dai, S.-T., Papamichos, E., 1996. Plane-strain compression of rock-like materials. Int. J. Rock. Mech. Min. Sci. & Geomech. Abstr. 33, 573–584.
Needleman, A., 1979. Non-normality and bifurcation in plane strain tension and compression. J. Mech. Phys. Solids 27, 231–254.
Ord, A., Vardoulakis, I., Kajewski, R., 1991. Shear band formation in Gosford sandstone. Int. J. Rock Mech. Min. Sci. & Geomech. Abstr. 28, 397–409.
Peng, S.D., 1971. Stresses within elastic circular cylinders loaded uniaxially and triaxially. Int. J. Rock Mech. Min. Sci. 8, 339–432.
Peng, S.D., 1973. Reply to discussion by M. Al-Chalabi 'On stresses within elastic cylinders loaded uniaxially and triaxially.' Int. J. Rock Mech. Min Sci. & Geomech. Abstr. 10, 761–762.
Pickett, G., 1994. Application of the Fourier method to the solution of certain boundary problems in the theory of elasticity. J. Appl. Mech. ASME 66, A176–A182.
Prager, W., Synge, J.L., 1947. Approximation in elasticity based on the concept of function space. Quart. Appl. Math. 5, 241–269.
Rudnicki, J.W., Rice, J.R., 1975. Conditions for the localization of deformation in pressure-sensitive dilatant materials. J. Mech. Phys. Solids 23, 371–394.
Stavropoulou, V.G., 1982. Behavior of brittle sandstone in plane-strain conditions. Proc. 23rd U.S. Symp. Rock Mech. Berkeley, California, pp. 351–358.
Tillard-Ngan, D., Desrues, J., Raynaud, S., Mazerolle, F., 1992. Strain localization in the Beaucaire Marl. In: Symposium on Mechanical Structure and Behaviour of Geomaterials, Nancy, France.
Vardoulakis, I., 1981. Bifurcation analysis of the plane strain rectilinear deformation on dry sand samples. Int. J. Solids Structures 17, 1085–1011.
Vardoulakis, I., Goldscheider, M., 1981. Biaxial apparatus for testing shear bands in soils. Proc. 10th Int. Conf. Soil Mech. Found. Engng., Stockholm, Balkema, Rotterdam, pp. 819–824.
Wawersik, W.R., Rudnicki, J.W., Olsson, W.A., Holcomb, D.J. and Chau, K.T., 1990. Localization of deformation in brittle rock: Theoretical and laboratory investigation. In: Shah, S.P., Swartz, S.E., Wang, M.L., (Eds) Micromechanics of Failure of Quasi-brittle Materials. Elsevier, pp. 115–124.
Watanabe, S., Discussion on 'Young's modulus interpreted from compression tests with end friction.' J. Eng. Mech. ASCE 124, 1170–1171.
Young, N.J.B., 1976. Bifurcation phenomena in the plane compression test. J. Mech. Phys. Solids 24, 77–91.